Evaluations of UAV-enabled FSO Communications in the Arctic

Sahil Nazir Pottoo[1], Pål Gunnar Ellingsen[1], Tu Dac Ho[1]

Abstract— **This paper investigates the feasibility of using free space optics (FSO) for communication between multiple hovering unmanned aerial vehicles (UAVs) and a detection unit (DU) in the Arctic. The uniqueness that sets apart UAV-based FSO systems from conventional FSO systems is the dynamics of the system since location and inclination of the UAV changes over time due to wind load and UAV oscillations. The envisioned scenario consists of UAVs equipped with laser diodes and a DU mounted on top of a ship. We propose an application scenario of search and rescue (SAR) operations in the High North. In the system design, the SAR team establishes communication with UAVs using radio frequency multiple-access links while DU demodulates the information from the incoming FSO fronthaul signals. Furthermore, statistical models for the FSO channel, random position and orientation fluctuations, snow, and fog have been derived. This work amplifies the need and possibility of enabling enhanced accessibility and connectivity in the Arctic utilizing UAVs and FSO.**

Keywords: ***Free space optical communications, unmanned aerial vehicles, channel modelling, Arctic weather.***

I. Introduction

Recently, unmanned aerial vehicles (UAVs), commonly known as drones have proven to be key elements in system integration. They are considered to be important in solving industrial or social challenges. UAVs offer a way to scan large maritime area in adverse weather conditions without risking human life, making them an important asset in search and rescue (SAR) operations in the Arctic [1], [2]. Together with the latest growth of autonomous systems, this has led to increased demand for developing new communication architectures for robust device-to-device connections.

As a consequence of climate change, the Arctic sea ice is melting. This melting has led to significant increase in ship traffic in recent years, increasing the need for SAR capabilities. It is anticipated that 80 million tonnes of freight will be shipped between Europe and Asia through the Northeast passage by 2025 and it would jump to 110 million tonnes by 2030 [3]. Today 80% of all Arctic shipping crosses Norwegian waters [4] and thereby through the Norwegian SAR area. The Arctic SAR agreement coordinates international SAR coverage and response in the Arctic. Norway's response area extends through the Barents Sea and Arctic Ocean up to the North Pole, covering an area many times larger than the total land area in Norway. Therefore, Norway has an important responsibility in increasing the emergency preparedness level and plan for future directions.

[1] Department of Electrical Engineering, Faculty of Engineering Science and Technology, UiT - The Arctic University of Norway,{Sahil.N.Pottoo, Pal.G.Ellingsen, Tu.D.Ho}@uit.no

The weather in the Barents Sea and Arctic Ocean can be very challenging for SAR operations. Moreover, the distances are vast, making SAR operations a gruelling task. Using UAVs as a part of the Norwegian SAR capacity mean that operations could be conducted more safely, quickly, and at a reduced cost. This requires high-speed uninterrupted connectivity between UAV-UAV, UAV-ground, and ground-UAV in order to transmit high resolution (multispectral) video data. Free space optics (FSO) appears a perfect candidate to establish data communication and networking between movable platforms.

Compared to radio frequency (RF) communications, FSO provides a large unlicensed THz spectrum, immunity to electromagnetic interference, high-level security, directional data fronthauling/backhauling, and ease of deployment at a relatively low cost [5], [6]. UAV-FSO integrated systems can be useful for civil applications, such as delivering wireless services across arctic regions or areas with a temporary large gathering like in sports matches or other live concerts, where permanent infrastructure is not available or is expensive to deploy [7], [8]. UAVs can hover above the designated region and operate as aerial base stations to employ FSO communication between the users and devices around [9]. UAVs monitor and collect useful data faster and at minimal cost than manned planes or helicopters [10]. UAV-FSO system can be implemented to carry out SAR operations by assisting in the execution where UAVs do 3D mapping of ocean floor/surface or land, and manned aircraft or ships do the rescuing. There remain significant technical challenges when flying and navigating UAVs in arctic conditions, but the technology is developing quickly, especially about improving the capacity to sustain extreme weather conditions, icing, and improve flight time [11].

This article will focus on the challenges of integrating UAVs into a communication system for arctic SAR or ship inspection setting. It will specifically look at the case of UAV-to-ground and ground-to-UAV communications. Autonomous UAVs in a rescue or inspections setting will be required to downlink a significant amount of data to the ship or ground based controller. We will investigate how the bit error rate and throughput of this downlink will be affected by the weather conditions expected in the Arctic with specific focus on the Barents sea.

II. System architecture

The proposed system is a UAV-based uplink/downlink transmission system in which mobile users connect with UAVs by RF multiple-access links (e.g. sub-6 GHz band)

and the detector unit (DU) receives FSO fronthaul signals as illustrated in Fig. 1. The focus of this paper is on SAR services in the Arctic. UAVs A and B are carrying laser diodes (LD) which direct laser beam to the DU mounted on the top of ship. An array of photodetectors (PDs) convert the received optical intensities in to baseband data. To avoid complicated link design, we have not used mechanical beam tracking at the DU. Instead, a lens has been placed in front of PDs that separates distinct incident spatial signals and guides them onto succeeding PDs [12], [13]. This structure also increases the overall detector surface area which enhances the probability of detection when UAVs A and B frequently change their positions [14]. In this case, the PDs are assumed to be ideal which means each PD is able to collect full optical power flux.

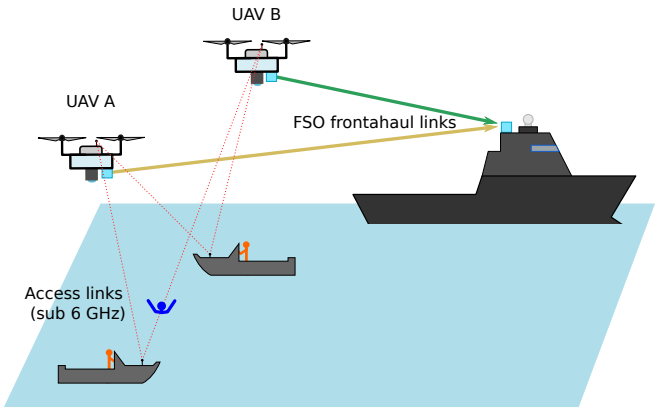

Fig. 1. The proposed architecture of a UAV-to-ship FSO system for SAR applications in the Arctic.

III. Statistical Modelling

To calculate the FSO channel characteristics under the Arctic weather conditions, several statistical models representing the degradation from turbulence, snow, and fog on FSO channel quality will be addressed. The effect of the changing position and orientation of a hovering UAV will also be investigated.

A. FSO channel model

An intensity modulation/direct detection (IM/DD) FSO system has been used where PD detects the received laser beam energy at logic 1 only [15]. Also, internal noise sources have been neglected and only the noise caused by solar energy is considered [16]. The received signal at the DU can then be expressed as [17]

$$y_s = hx_s + n, \tag{1}$$

where $x_s \in R^+$ is irradiance, $n \in R$ is real-valued additive white Gaussian noise having variance σ_n^2 and $h \in R^+$ signifies the channel coefficient.

The bit error rate (BER) of the received signal can be expressed as [18]

$$BER = \frac{\text{erfc}}{2}\left(\sqrt{\frac{E_b}{2\sigma_n^2}}\right) \tag{2}$$

where $E_b = a_2^i = 1$ is the normalized bit energy. Considering ϵ-outage capacity is the largest transmission rate so that the outage probability is less than ϵ and is written as [19]

$$C_\epsilon = \max\{R : P_o(R) \leq \epsilon\}, \tag{3}$$

where $R : P_o(R)$ is the outage probability, then the throughput which represents maximum successful transmission to the DU is given by

$$T_\epsilon = (1-\epsilon)C_\epsilon. \tag{4}$$

An average power constraint $E\{x_s\} \leq P$ (transmitted power) also applies. The h is affected by many states which can be expressed as [14]

$$h = \nu h_p h_a h_g, \tag{5}$$

where ν is the responsivity and h_p, h_a, and h_g denote atmospheric loss, atmospheric fading, and geometric and misalignment losses (GML), respectively. In particular, atmospheric loss, h_p, is deterministic and gives the power loss on a transmission path due to absorption and scattering. It is modelled as [20]

$$h_p = 10^{-\kappa L/10}, \tag{6}$$

where L in meter is separation between UAV and DU and κ [m^{-1}] represents the attenuation constant for the FSO system. The atmospheric turbulence, h_a, is a random variable (RV) and induced by inhomogeneity of the air temperature and pressure. It is modelled as log-normal (LN) and Gamma-Gamma (GG) distributed RV for weak and moderate turbulence channels [13]. We assume that turbulence is moderate at the taken altitude, and its consequences are negligible in comparison to GML. To prove this assertion, a negative GG model, i.e., $h_a \sim \text{GG}(\alpha, \beta)$, with fading parameters α and β can be used. For GG fading, h_a is modelled as the product of two separate Gamma RVs $h_a^{(1)} \sim \text{G}(\alpha, \alpha)$ and $h_a^{(2)} \sim \text{G}(\beta, \beta)$, which represent fluctuations due to large- and small-scale fading, respectively [21]. Parameters α and β are the inverse of the variances of $h_a^{(1)}$ and $h_a^{(2)}$, and are given by [22]

$$\alpha = \left[\exp\left(\frac{0.49\sigma_R^2}{\left(1+1.11\sigma_R^{12/5}\right)^{7/6}} - 1\right)\right]^{-1}, \tag{7}$$

$$\beta = \left[\exp\left(\frac{0.51\sigma_R^2}{\left(1+0.69\sigma_R^{12/5}\right)^{5/6}} - 1\right)\right]^{-1}. \tag{8}$$

$\sigma_R^2 = 1.23 C_n^2 k^{7/6} L^{11/6}$ is the Rytov variance, $k = 2\pi/\lambda$, where λ [m] denotes the optical wavelength, and

$$C_n^2 \approx C_0^2 \exp\left(-\frac{h_d}{100}\right)\left[\text{m}^{-2/3}\right], \tag{9}$$

is refraction index. h_d is UAV height and $C_0^2 = 1.7 \times 10^{-14}$ $\text{m}^{-2/3}$ is the nominal value of refractive index on

ground [23]. Therefore, we estimate h_a by its mean value, i.e.

$$h_a \approx E\{h_a\} \approx E\{h_a^1\}E\{h_a^2\} = \frac{\alpha}{\alpha} \times \frac{\beta}{\beta} = 1. \tag{10}$$

GML, h_g, is generated due to laser beam divergence between the transmitting and the receiving lenses, and the misalignment between the beam and the center of the lens [24]. Inconsistencies in the placement and orientation of the UAV yield to a random h_g given by [17]

$$h_g(\mathbf{r}, \boldsymbol{\omega}) = \iint\limits_{(y,z)\in\mathcal{A}} I(y,z)\mathrm{d}y\mathrm{d}z, \tag{11}$$

where $I(y,z)$ is power density at point (y,z) on the PD plane and A is the set of (y,z) within the lens area.

B. Models for position and orientation changes of hovering UAVs

It becomes difficult to maintain line-of-sight for an effective FSO transmission between the UAVs and the DU because the UAVs were hovering in the air and the motion of the ship on sea. Therefore, a proper dynamic control mechanism is required to maintain orientation of the laser beam precisely so that center of the laser beam should coincide with the center of the receiver lens [25]. Also, in UAVs, there is an error linked with wind estimation [26], and the wind effect is therefore not fully compensated [25]. For UAV-FSO system, tracking errors are expected to be more critical due to high mobility and instability of the UAVs. We define $\mu_r = (\mu_x, \mu_y, \mu_z)$ and $\mu_\omega = (\mu_\theta, \mu_\phi)$ as the means of random vectors $\vec{r}$ and $\vec{\omega}$, and $\epsilon_r = (\epsilon_x, \epsilon_y, \epsilon_z)$ and $\epsilon_\omega = (\epsilon_\theta, \epsilon_\phi)$ as the zero-mean random vectors which model the variations in the position and orientation of the UAV. On this account the location and orientation of the UAV can be expressed as follows [17]

$$\vec{r} = \mu_r + \epsilon_r, \vec{\omega} = \mu_\omega + \epsilon_\omega. \tag{12}$$

Because GML is dependent on ϵ_r and ϵ_ω, the distribution of ϵ_r and ϵ_ω decides the distribution of GML. Hence, embracing correct distributions for variations ϵ_r and ϵ_ω is necessary for developing a practical mathematical model for the GML. Beacause UAVs hover above the users, μ_r depends on the location of the users as well as the UAV height. Given μ_r, the tracking mechanism aims to calculate μ_ω in a way that the laser beam cuts across the center of the DU lens, so that the lens collects greater power. This gives the first moment RVs [17]

$$\mu_\theta = \begin{cases} \pi + \tan^{-1}\frac{\mu_y}{\mu_x} & \mu_x > 0 \\ \tan^{-1}\frac{\mu_y}{\mu_x} & \text{otherwise} \end{cases} \tag{13}$$

$$\mu_\phi = \pi - \cos^{-1}\frac{\mu_z}{\sqrt{\mu_x^2 + \mu_y^2 + \mu_z^2}}. \tag{14}$$

We can now say, $E\{\vec{b}\} = (0,0,0)$. The second moments of $\vec{r}$ and $\vec{\omega}$ determine stability of the UAV over the mean values μ_r and μ_ω. Specifically, the less the variances of the vectors $\vec{r}$ and $\vec{\omega}$ are, further stable the UAV becomes.

C. Modeling effects of snow on a FSO link

One of the weather conditions which will effect the FSO link in the Arctic is snow. The attenuation caused by snow is highly variational and depends on the density and size of snow crystals. FSO links through snow are affected and degraded in a major way due to the signal attenuation [27]. The attenuation coefficient is given by [28]

$$\gamma = as^b, \tag{15}$$

where γ represents the attenuation in $\mathrm{dB/km}$ due to snow, s is the rate of snowfall in mm/hour and a, b are constants dependent upon the physical characteristics of snow.

D. Modeling effects of fog on a FSO link

Fog is a common occurrence in the High North which also reduces visibility considerably. The attenuation caused by fog on a FSO link is significant. It may cause attenuation of up to hundreds of $\mathrm{dB/km}$. Hence, accurate modelling of fog attenuation and visibility will help SAR providers to engineer and appropriately manage rescue operations. Based on the model in [29], a mathematical model for fog is expressed as follows

$$q = \begin{cases} 1.6 & V > 50\,\mathrm{km} \\ 1.3 & 6\,\mathrm{km} < V < 50\,\mathrm{km} \\ 0.16V + 0.34 & 1\,\mathrm{km} V < 6\,\mathrm{km} \\ V - 0.5 & 0.5\,\mathrm{km} V < 50\,\mathrm{km} \\ 0 & V < 0.5\,\mathrm{km} \end{cases} \tag{16}$$

where V is the visibility in km and q is measure of particle size distribution in free-space. This model suggests that $550\,\mathrm{nm}$ and $1550\,\mathrm{nm}$ optical windows will undergo same attenuation for visibility less than $500\,\mathrm{m}$.

IV. Simulations and case study of UAV-Ship enabled FSO system in Barents Sea

In order to model exact link performance, it is appropriate to work out what weather conditions one would expect to encounter in the Barents Sea. The Norwegian Meteorological Institute (MET Norway) has two operational weather stations on islands in the Barents Sea. One is located on Hopen, southeast of Svalbard at 76.5097°N and 25.0133°E, and the other on Bjørnøya, located roughly midway between Norway and Svalbard at 74.5025°N and 18.988°E.

Fig. 2 illustrates average monthly observed variations in weather conditions on Hopen and Bjørnøya from 2000 to 2021. In Fig. 3, the same data for october 2020-21 is shown in order to highlight past 12 months weather statistics. The weather parameters most relevant to the Arctic such as temperature, cloud cover, wind, visibility, and snow cover have been considered in the proposed design and analysis. These statistics reveal the picture of expected climate in and around the Barents Sea. On comparing data from Figures 2 and 3, it is noted that generally temperature remains between $0\,^\circ\mathrm{C}$ to $-10\,^\circ\mathrm{C}$, thick cloud cover is present that means low visibility, average 10 m/s wind speed is recorded which can

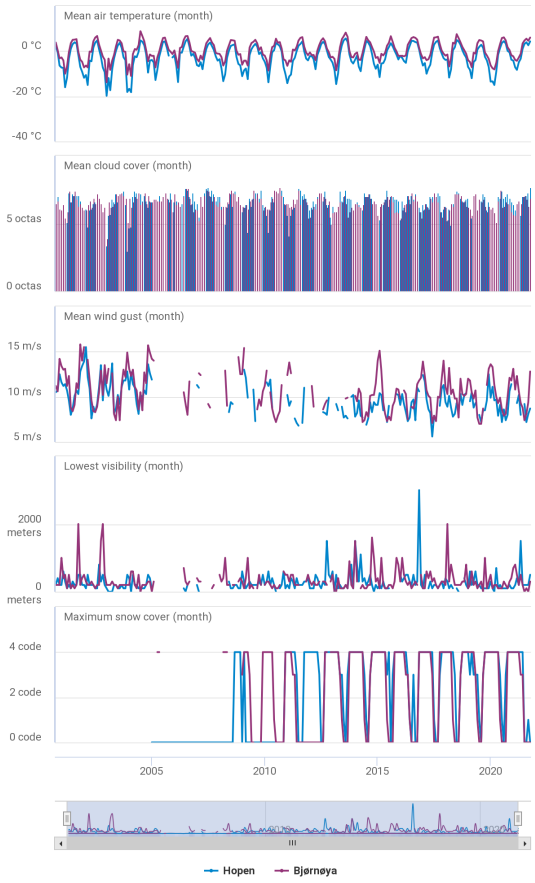

Fig. 2. The monthly variation in temperature, cloud coverage, wind, visibility and snow from observations at the meteorological stations on Bjørnøya (purple) and Hopen (blue) over the time frame from October 2000 to October 2021. Data and plots courtesy of The Norwegian Meteorological Institute [30].

Fig. 3. The monthly variation in temperature, cloud coverage, wind, visibility and snow from observations at the meteorological stations on Bjørnøya (purple) and Hopen (blue) over a year from October 2020 to October 2021. Data and plots courtesy of The Norwegian Meteorological Institute [30].

cause misalignment issues between the UAVs and DU, and usually deep snow cover exists.

For the FSO channel performance evaluations, the simulations have applied all the parameters defined in Table I and used weather statistics from Figures 2 and 3. The BER and throughput have been calculated using equations (2) and (4). The values out of numerical evaluations match with the one's obtained from simulation software. Fig. 4 depicts FSO link throughput evaluation with increasing UAV altitude. The throughput (in Gbps) at 0, 60, 120 m UAV altitude in clear (sunny) weather is 10, 9.6, and 8.8; in wind it is 9.1, 7.5, and 6.5; in snow it is 6.1, 4.8, and 4.1; in fog it is 2.6, 1.7, and in coexistent wind and snow it is 0.7, 0.4, and 0. This result reveals that throughput is deteriorated with an increase in UAV height and is lowest when both wind and snow are present and in fog, moderate in snow and wind, and highest in clear environments. Fig. 5 shows the BER performance of the proposed FSO link with increasing coverage area for most prevalent Arctic weather conditions. The highest BER at maximum transmission range of 2000 m in clear weather is -8.7; in wind it is -5.5; in snow it is -3; in fog it is -1, and in both wind and snow it is 0 (i.e. no communication possible). Therefore, simultaneous wind and snow has caused highest BER. Other climate scenarios have shown low BER at less range and acceptable BER at greater distances which proves reliable FSO communication is possible.

V. Conclusions

We have investigated a UAV-enabled FSO communication system that could enable a wideband data link with a supporting vessel, for instance, in a SAR operation in the Arctic. The statistical models for FSO channel performance under different weather conditions, random position and direction of UAVs were also presented. Based on the latest year and two-decade-old weather data sets from Hopen and Bjørnøya stations in Northern Norway, the most prevailing weather conditions in the Arctic were visualized and applied to the simulations. From the channel throughput and BER evaluations, it is concluded that coexistent wind and snow had the most severe effect on FSO link performance followed by fog, snow, and wind, separately. The simulations also included sunny or clear weather scenario to put forward direct comparison with other climatic conditions in the Arctic and demonstrate the extent of atmospheric effects on FSO communication system.

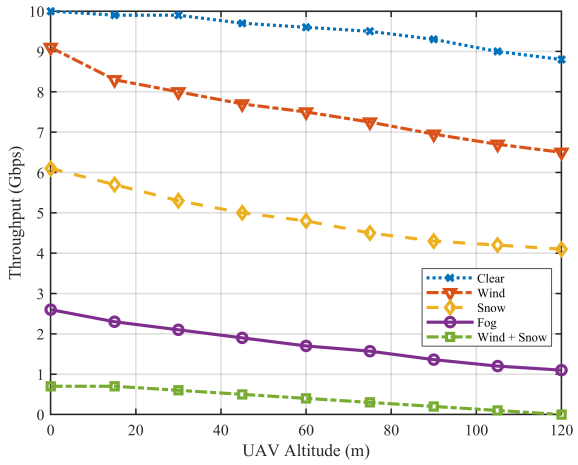

Fig. 4. Variation of the network throughput as a function of weather condition and UAV altitude.

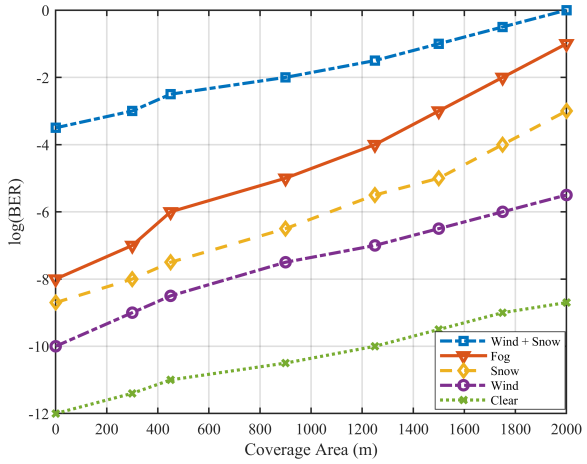

Fig. 5. Variation of log BER as a function of range and weather condition.

In future work, a prototype of the proposed system will be developed and investigated in the laboratory with artificial snow and icing conditions similar to the Arctic conditions used here. On completion of this testing, a measurement campaign in Narvik (68.438 499°N and 17.427 261°E) will be conducted. In addition, a weather-based dynamic relaying mechanism for the FSO through swarm of UAVs for mitigating atmospheric and geometrical effects will be proposed.

Parameter	Value
Wavelength	1550 nm
Input power	10 dBm
Coverage area	0 m to 2000 m
Lens radius	0.05 m
APD gain	1
Electrical bandwidth of APD	1 GHz
APD load resistance	1 kΩ
Detector noise temperature	300 K
Ionization factor	0.7
Receiver aperture diameter	0.09 m
Receiver FOV angle	20 mrad
Laser linewidth	0.1 MHz
Maximum throughput	10 Gbps
Beam divergence angle	0.25 mrad
APD responsivity	1 A/W
Pointing loss	2 dB
Elevation angle	45°
Maximum UAV altitude	120 m
Wind speed	12 m/s
Receiver sensitivity	100 photons/bit
Optical efficiency of transmitter	0.75
Optical efficiency of receiver	0.75
APD dark current	10 nA
Noise figure	1
Avalanche multiplication factor	40
Receiver loss	1 dB
Noise variance	∼ 225 dBm/Hz
Snow rate	30 mm/h
Visibility	500 m
Average fog attenuation	150 dB/km
Average snow attenuation	90 dB/km

TABLE I

THE VALUES OF THE PARAMETERS USED IN THE SIMULATIONS.

REFERENCES

[1] X. Zhong, Y. Guo, N. Li, and Y. Chen, "Joint Optimization of Relay Deployment, Channel Allocation, and Relay Assignment for UAVs-Aided D2D Networks," *IEEE/ACM Transactions on Networking*, vol. 28, no. 2, pp. 804–817, 2020, ISSN: 15582566. DOI: 10.1109/TNET.2020.2970744.

[2] J. H. Lee, K. H. Park, Y. C. Ko, and M. S. Alouini, "Throughput Maximization of Mixed FSO/RF UAV-Aided Mobile Relaying with a Buffer," *IEEE Transactions on Wireless Communications*, vol. 20, no. 1, pp. 683–694, 2021, ISSN: 15582248. DOI: 10.1109/TWC.2020.3028068. arXiv: 2001.01193.

[3] H. Kubny, *New record in the Northeast Passage*, 2020. [Online]. Available: https://polarjournal.ch/en/2020/10/21/new-record-in-the-northeast-passage/ (visited on 10/06/2021).

[4] Det Kongelige Samferdselsdepartement, "Meld. St. 31 (2015–2016) Postsektoren i endring," Det Kongelige Samferdselsdepartement, Tech. Rep., 2016, p. 56. [Online]. Available: https://www.regjeringen.no/no/dokumenter/meld.-st.-31-20152016/id2499743/.

[5] S. Zhang and N. Ansari, "3D Drone Base Station Placement and Resource Allocation with FSO-Based Backhaul in Hotspots," *IEEE Transactions on Vehicular Technology*, vol. 69, no. 3, pp. 3322–3329, 2020, ISSN: 19399359. DOI: 10.1109/TVT.2020.2965920.

[6] Z. Gu, J. Zhang, X. Sun, and Y. Ji, "Optimizing Networked Flying Platform Deployment and Access Point Association in FSO-Based Fronthaul Networks," *IEEE Wireless Communications Letters*, vol. 9, no. 8, pp. 1221–1225, 2020, ISSN: 21622345. DOI: 10.1109/LWC.2020.2986406.

[7] S. Hayat, E. Yanmaz, and R. Muzaffar, "Survey on Unmanned Aerial Vehicle Networks for Civil Applications: A Communications Viewpoint," *IEEE Communications Surveys and Tutorials*, vol. 18, no. 4, pp. 2624–2661, 2016, ISSN: 1553877X. DOI: 10.1109/COMST.2016.2560343.

[8] Y. Dong, M. Z. Hassan, J. Cheng, M. J. Hossain, and V. C. Leung, "An edge computing empowered radio access network with UAV-Mounted FSO fronthaul and backhaul: Key challenges and approaches," *IEEE Wireless Communications*, vol. 25, no. 3, pp. 154–160, 2018, ISSN: 15361284.

DOI: 10.1109/MWC.2018.1700419. arXiv: 1803.06381.

[9] M. Kishk, A. Bader, and M. S. Alouini, "Aerial Base Station Deployment in 6G Cellular Networks Using Tethered Drones: The Mobility and Endurance Tradeoff," *IEEE Vehicular Technology Magazine*, vol. 15, no. 4, pp. 103–111, 2020, ISSN: 15566080. DOI: 10.1109/MVT.2020.3017885. arXiv: 1906.11559.

[10] Y. L. Che, W. Long, S. Luo, K. Wu, and R. Zhang, "Energy-Efficient UAV Multicasting with Simultaneous FSO Backhaul and Power Transfer," *IEEE Wireless Communications Letters*, vol. 10, no. 7, pp. 1537–1541, 2021, ISSN: 21622345. DOI: 10.1109/LWC.2021.3073477. arXiv: 2104.03048.

[11] Teknologirådet, *Drones in the Arctic*, 2013. [Online]. Available: https://teknologiradet.no/en/drones-in-the-arctic/ (visited on 10/06/2021).

[12] I. Grishin, V. Vishnevsky, T. D. Dinh, A. Vybornova, and R. Kirichek, "Methods for correcting positions of tethered UAVs in adverse weather conditions," *International Congress on Ultra Modern Telecommunications and Control Systems and Workshops*, vol. 2020-October, pp. 308–312, 2020, ISSN: 2157023X. DOI: 10.1109/ICUMT51630.2020.9222424.

[13] L. Li, R. Zhang, Z. Zhao, G. Xie, P. Liao, K. Pang, H. Song, C. Liu, Y. Ren, G. Labroille, P. Jian, D. Starodubov, B. Lynn, R. Bock, M. Tur, and A. E. Willner, "High-Capacity Free-Space Optical Communications between a Ground Transmitter and a Ground Receiver via a UAV Using Multiplexing of Multiple Orbital-Angular-Momentum Beams," *Scientific Reports*, vol. 7, no. 1, pp. 1–12, 2017, ISSN: 20452322. DOI: 10.1038/s41598-017-17580-y. [Online]. Available: http://dx.doi.org/10.1038/s41598-017-17580-y.

[14] A. A. Farid and S. Hranilovic, "Outage capacity optimization for free-space optical links with pointing errors," *Journal of Lightwave Technology*, vol. 25, no. 7, pp. 1702–1710, 2007, ISSN: 07338724. DOI: 10.1109/JLT.2007.899174.

[15] S. K. Khan, U. Naseem, A. Sattar, N. Waheed, A. Mir, A. Qazi, and M. Ismail, "Uav-aided 5g network in suburban, urban, dense urban, and high-rise urban environments," in *2020 IEEE 19th International Symposium on Network Computing and Applications (NCA)*, 2020, pp. 1–4. DOI: 10.1109/NCA51143.2020.9306710.

[16] X. Zhu and J. M. Kahn, "Survey on free space optical communication: A communication theory perspective," *IEEE Transactions on Communications*, vol. 16, no. 4, pp. 2231–2258, 2014, ISSN: 00906778. DOI: 10.1109/TCOMM.2002.800829.

[17] M. Najafi, H. Ajam, V. Jamali, P. D. DIamantoulakis, G. K. Karagiannidis, and R. Schober, "Statistical Modeling of the FSO Fronthaul Channel for UAV-Based Communications," *IEEE Transactions on Communications*, vol. 68, no. 6, pp. 3720–3736, 2020, ISSN: 15580857. DOI: 10.1109/TCOMM.2020.2981560.

[18] M. T. Dabiri, S. M. S. Sadough, and H. Savojbolaghchi, "Achieved Throughput of Hovering UAV-Based Optical Wireless Communications," *3rd West Asian Symposium on Optical and Millimeter-Wave Wireless Communications, WASOWC 2020*, no. Wasowc, 2020. DOI: 10.1109/WASOWC49739.2020.9410024. arXiv: 2106.15263.

[19] S. Zhalehpour, M. Uysal, O. A. Dobre, and T. Ngatched, "Outage capacity and throughput analysis of multiuser FSO systems," in *2015 IEEE 14th Canadian Workshop on Information Theory (CWIT)*, IEEE, Jul. 2015, pp. 143–146, ISBN: 978-1-4799-6560-1. DOI: 10.1109/CWIT.2015.7255172. [Online]. Available: http://ieeexplore.ieee.org/document/7255172/.

[20] V. Jamali, D. S. Michalopoulos, M. Uysal, and R. Schober, "Link Allocation for Multiuser Systems With Hybrid RF/FSO Backhaul: Delay-Limited and Delay-Tolerant Designs," *IEEE Transactions on Wireless Communications*, vol. 15, no. 5, pp. 3281–3295, 2016, ISSN: 15361276. DOI: 10.1109/TWC.2016.2519508.

[21] J.-Y. Wang, Y. Ma, R.-R. Lu, J.-B. Wang, M. Lin, and J. Cheng, "Hovering UAV-Based FSO Communications: Channel Modelling, Performance Analysis, and Parameter Optimization," pp. 1–14, 2021. arXiv: 2104.05368. [Online]. Available: http://arxiv.org/abs/2104.05368.

[22] H. Alquwaiee, H. C. Yang, and M. S. Alouini, "On the asymptotic capacity of dual-aperture FSO systems with generalized pointing error model," *IEEE Transactions on Wireless Communications*, vol. 15, no. 9, pp. 6502–6512, 2016, ISSN: 15361276. DOI: 10.1109/TWC.2016.2585486.

[23] W. Khawaja, I. Guvenc, D. W. Matolak, U. C. Fiebig, and N. Schneckenburger, "A Survey of Air-to-Ground Propagation Channel Modeling for Unmanned Aerial Vehicles," *IEEE Communications Surveys and Tutorials*, vol. 21, no. 3, pp. 2361–2391, 2019, ISSN: 1553877X. DOI: 10.1109/COMST.2019.2915069. arXiv: 1801.01656.

[24] M. T. Dabiri, S. M. S. Sadough, and M. A. Khalighi, "Channel modeling and parameter optimization for hovering UAV-Based free-space optical links," *IEEE Journal on Selected Areas in Communications*, vol. 36, no. 9, pp. 2104–2113, 2018, ISSN: 15580008. DOI: 10.1109/JSAC.2018.2864416.

[25] N. Amari, D. Folio, and A. Ferreira, "Robust laser beam tracking control using micro/nano dual-stage manipulators," *IEEE International Conference on Intelligent Robots and Systems*, pp. 1543–1548, 2013, ISSN: 21530858. DOI: 10.1109/IROS.2013.6696554.

[26] Y. Song, B. Luo, and Q. H. Meng, "A rotor-aerodynamics-based wind estimation method using a quadrotor," *Measurement Science and Technology*, vol. 29, no. 2, 2018, ISSN: 13616501. DOI: 10.1088/1361-6501/aa8a9d.

[27] H. S. Khallaf, K. Kato, E. M. Mohamed, S. M. Sait, H. Yanikomeroglu, and M. Uysal, "Composite Fading Model for Aerial MIMO FSO Links in the Presence of Atmospheric Turbulence and Pointing Errors," *IEEE Wireless Communications Letters*, vol. 10, no. 6, pp. 1295–1299, 2021, ISSN: 21622345. DOI: 10.1109/LWC.2021.3064832.

[28] B. Wang, Z. A. Ali, and D. Wang, "Controller for UAV to Oppose Different Kinds of Wind in the Environment," *Journal of Control Science and Engineering*, vol. 2020, 2020, ISSN: 16875257. DOI: 10.1155/2020/5708970.

[29] M. A. Esmail, H. Fathallah, and M. S. Alouini, "Outdoor FSO Communications under Fog: Attenuation Modeling and Performance Evaluation," *IEEE Photonics Journal*, vol. 8, no. 4, pp. 1–22, 2016, ISSN: 19430655. DOI: 10.1109/JPHOT.2016.2592705.

[30] T. N. M. I. (Norway), *Observations and weather statistics*, 2021. [Online]. Available: https://seklima.met.no/observations/ (visited on 10/06/2021).